Geomechanics and Engineering, *Vol. 10, No. 3 (2016) 357-386*
DOI: http://dx.doi.org/10.12989/gae.2016.10.3.357

Thermal stability analysis of solar functionally graded plates on elastic foundation using an efficient hyperbolic shear deformation theory

Sidi Mohamed El-Hassar [1], Samir Benyoucef [1,2,3], Houari Heireche [4] and Abdelouahed Tounsi [*1]

[1] *Laboratoire des Structures et Matériaux Avancés dans le Génie Civil et Travaux Publics, Université de Sidi Bel Abbes, Faculté de Technologie, Département de Génie Civil, Algeria*
[2] *Material and Hydrology Laboratory, University of Sidi Bel Abbes, Faculty of Technology, Civil Engineering Department, Algeria*
[3] *Algerian National Thematic Agency of Research in Science and Technology (ATRST), Algeria*
[4] *Laboratoire de Modélisation et Simulation Multi-échelle, Département de Physique, Faculté des Sciences Exactes, Département de Physique, Université de Sidi Bel Abbés, Algeria*

(*Received November 05, 2015, Revised December 23, 2015, Accepted December 29, 2015*)

Abstract. In this research work, an exact analytical solution for thermal stability of solar functionally graded rectangular plates subjected to uniform, linear and non-linear temperature rises across the thickness direction is developed. It is assumed that the plate rests on two-parameter elastic foundation and its material properties vary through the thickness of the plate as a power function. The neutral surface position for such plate is determined, and the efficient hyperbolic plate theory based on exact neutral surface position is employed to derive the governing stability equations. The displacement field is chosen based on assumptions that the in-plane and transverse displacements consist of bending and shear components, and the shear components of in-plane displacements give rise to the quadratic distribution of transverse shear stress through the thickness in such a way that shear stresses vanish on the plate surfaces. Therefore, there is no need to use shear correction factor. Just four unknown displacement functions are used in the present theory against five unknown displacement functions used in the corresponding ones. The non-linear strain-displacement relations are also taken into consideration. The influences of many plate parameters on buckling temperature difference will be investigated. Numerical results are presented for the present theory, demonstrating its importance and accuracy in comparison to other theories.

Keywords: thermal buckling; solar functionally graded plate; analytical modeling; neutral surface position

1. Introduction

Solar plate is employed to concentrate solar radiation onto an absorber positioned at the focal point in parabolic dish concentrator to provide the solar energy. Concentrating solar collector is composed of reflector over solar plate, the absorber and the housing. Parabolic disk fabricated from solar plates. The performance of a solar plate in terms efficiency, service life and optical

*Corresponding author, Professor, E-mail: tou_abdel@yahoo.com

http://www.techno-press.org/?journal=gae&subpage=7 ISSN: 2005-307X (Print), 2092-6219 (Online)

alignment depends on the material and operating conditions. Normally, a solar plate can be manufactured from polished pure material or coated plate with some special cover (Howell and Bereny 1979). However, for some specific application, such as in solar satellite, solar power tower and solar power heat engine can demand low weight and high temperature environment. High thermal resistance provides suitable stiffness to avoid unsought deformation to better optical alignment. Such plates need to be manufactured using special material such as a functionally graded material (FGM) with steel and ceramic combined together (Shahrjerdi *et al*. 2010, Khalfi *et al*. 2014, Hadji *et al*. 2014, Tounsi *et al*. 2013, Bouderba *et al*. 2013, Attia *et al*. 2015).

A plentiful number of plates resting on elastic foundation are important in structural engineering and have wide application in other engineering fields. Such plate structures can be found in various kinds of industrial applications like raft foundations, storage tanks, swimming pools, and in most civil engineering constructions. To describe the interaction between the plate and foundation, various kinds of foundation models have been proposed. The simplest one is Winkler or one-parameter model (Winkler 1867). However, Winkler's model is unable to take into account the continuity or cohesion of the soil. Also, the assumption that there is no interaction between adjacent springs results in ignoring the influence of the soil on either side of the beam. To overcome this weakness, many two-parameter elastic foundation models have been proposed, such as Pasternak (Pasternak 1954) by adding a shear spring to simulate the interactions between the separated springs in the Winkler model. The Pasternak or two-parameter model is widely used to describe the mechanical behavior of structure-foundation interactions. Benyoucef *et al*. (2010) investigated the bending response of thick functionally graded plates resting on Pasternak's elastic foundations. Ait Atmane *et al*. (2010) presented a free vibration analysis of a functionally graded plate resting on a two-parameter elastic foundation using a new shear deformation plate theory. Kiani and Eslami (2012) studied the thermal buckling and post-buckling response of imperfect temperature-dependent sandwich FG plates resting on elastic foundation. Sobhy (2013) investigated the buckling and free vibration of exponentially graded sandwich plates resting on elastic foundations under various boundary conditions. Zidi *et al*. (2014) studied the hygro-thermo-mechanical bending response of FG plate resting on elastic foundations. Ait Amar Meziane *et al*. (2014) studied the bending and vibration behaviour of exponentially graded sandwich plates under various boundary conditions and resting on elastic foundations. Zenkour *et al*. (2014) studied the influence of temperature and moisture on the bending behavior of composite FG plates resting on elastic foundations. Yaghoobi *et al*. (2014) presented an analytical study on post-buckling and nonlinear free vibration analysis of FG beams resting on nonlinear elastic foundation under thermo-mechanical loadings using VIM. Tebboune *et al*. (2015) discussed the thermal buckling behavior of FG plates resting on elastic foundation based on an efficient and simple trigonometric shear deformation theory. Bounouara *et al*. (2016) investigated the free vibration of FG nanoscale plates resting on elastic foundation using a nonlocal zeroth-order shear deformation theory. Salima *et al*. (2016) studied the free vibration of FG rectangular plates on Winkler–Pasternak elastic foundations using an efficient and simple shear deformation theory.

In conventional laminated composite structures, homogeneous elastic laminates are bonded together to obtain enhanced mechanical and thermal properties (Draiche *et al*. 2014, Chattibi *et al*. 2015). However, the abrupt change in material properties across the interface between different materials can result in large inter-laminar stresses leading to delamination, cracking, and other damage mechanisms which result from the abrupt change of the mechanical properties at the interface between the layers. To remedy such defects, functionally graded materials (FGMs) within which material properties vary continuously, have been proposed (Koizumi 1997). Solar plate is

employed to focus solar radiation onto an absorber located at the focal point in parabolic dish concentrator to give the solar energy. Concentrating solar collector consists of reflector over solar plate, the absorber and the housing. Parabolic disk is fabricated from solar plates. The performance of a solar plate in terms efficiency, service life and optical alignment depends on the material and operating conditions. Normally, a solar plate can be made from polished pure material or coated plate with some special cover (Howell and Bereny 1979). However, for some specific application, such as in solar satellite, solar power tower and solar power heat engine can demand low weight and high temperature environment. High thermal resistance provides suitable stiffness to avoid unsought deformation to better optical alignment. Such plates need to be manufactured by employing special material such as a functionally graded material (FGM) with steel and ceramic combined together (Shahrjerdi *et al*. 2010). The mechanical behavior of structural components with FGMs is of highly importance in both research and industrial fields (Talha and Singh 2010, Belabed *et al*. 2014, Benachour *et al*. 2011, Pradhan and Chakraverty 2015, Ait Yahia *et al*. 2015, Arefi 2015, Bennai *et al*. 2015, Sallai *et al*. 2015, Tagrara *et al*. 2015, Ebrahimi and Dashti 2015, Belkorissat *et al*. 2015, Mahi *et al*. 2015, Ait Atmane *et al*. 2015, Kar and Panda 2015, Larbi Chaht *et al*. 2015, Zenkour and Abouelregal 2015, Darılmaz 2015, Bennoun *et al*. 2016, Ait Atmane *et al*. 2016). Bourada *et al*. (2012) presented a new four-variable refined plate theory for thermal buckling analysis of FG sandwich plates. Hamidi *et al*. (2015) proposed a sinusoidal plate theory with 5-unknowns and stretching effect for thermo-mechanical bending of FG sandwich plates. Bouchafa *et al*. (2015) studied the thermal stresses and deflections of FG sandwich plates using a new refined hyperbolic shear deformation theory. Akbaş (2015) presented an elastic solution of a curved beam made of functionally graded materials with different cross sections. Nguyen *et al*. (2015) examined the bending, vibration and buckling responses of FG sandwich plates using refined higher-order shear deformation theory.

The solar functionally graded plates (SFGPs) are commonly employed in thermal environments; they can buckle under thermal and mechanical loads. Thus, the buckling investigation of such plates is essential to ensure an efficient and reliable design. By using an analytical approach, they obtained closed-form expressions for buckling loads. Shahrjerdi *et al*. (2010) used second order shear deformation theory to analyze stress distribution for solar functionally graded plates. Using also the second-order shear deformation theory, Shahrjerdi *et al*. (2011a, b) analyzed the vibration of temperature-dependent solar FG plates. Lanhe (2004) analyzed the critical temperature and critical temperature difference of simply supported moderately thick rectangular FG plates on the basis of the first-order shear deformation theory in the Von Karman sense. For moderately thick FG plates, it has been pointed out that transverse shear deformation has considerable effects on the critical buckling temperature difference. Thermal buckling of simply supported FG skew plates has been investigated using the first-order shear deformation theory by Ganapathi and Prakash (2006). The effects of aspect and thickness ratios, gradient index and skew angle on the critical temperature difference were presented. Na and Kim (2006) investigated the thermal postbuckling of FGM plates by using the three-dimensional finite-element method. Zhao *et al*. (2009) and Zhao and Liew (2009) analyzed the buckling and postbuckling behavior of FGM plates by invoking the element-free kp-Ritz method. Matsunaga (2009) presented a higher order deformation theory for thermal buckling of FGM plates. By using the method of power series expansion of displacement components, a set of fundamental equations of rectangular FGM plates was derived. The trigonometric shear deformation plate theory was employed by Zenkour and Sobhy (2011) to study the thermal buckling of FGM plates on two-parameter elastic foundation. Bouazza *et al*. (2010) investigated the thermoelastic buckling of FGM plate using first shear plate theory. Effects of

changing plate characteristics, material composition and volume fraction of constituent materials on the critical temperature difference of FGM plate with simply supported edges are also investigated. Yaghoobi and Torabi (2013) presented an exact solution for thermal buckling of FG plates resting on elastic foundations with various boundary conditions. Akil (2014) studied the post-buckling response of sandwich beams with FG faces using a consistent higher order theory. Bakora and Tounsi (2015) examined the thermo-mechanical post-buckling behavior of FG plates resting on Pasternak-type elastic foundation. Hadji *et al*. (2015) presented an *n*-order four variable refined theory for thermal buckling analysis of FG plates.

Since, the material properties of functionally graded plate vary through the thickness direction, the neutral surface of such plate may not coincide with its geometric middle surface. Therefore, stretching and bending deformations of FGM plate are coupled. Some researchers (Morimoto *et al*. 2006, Abrate 2008, Zhang and Zhou 2008, Saidi and Jomehzadeh 2009, Ould Larbi *et al*. 2013, Bousahla *et al*. 2014, Fekrar *et al*. 2014, Bourada *et al*. 2015) have shown that there is no stretching-bending coupling in constitutive equations if the reference surface is properly selected.

This paper aims to develop an efficient hyperbolic shear deformation theory based on exact position of neutral surface for thermal buckling analysis of FGM plates resting on two-parameter elastic foundation. By introducing the physical neutral surface the stretching-bending coupling terms in the governing differential equations were eliminated. This theory is based on assumption that the in-plane and transverse displacements consist of bending and shear components in which the bending components do not contribute toward shear forces and, likewise, the shear components do not contribute toward bending moments. Just four unknown displacement functions are used in the present theory against five unknown displacement functions used in the corresponding ones. The material properties are graded in the thickness direction according to the power-law distribution in terms of volume fractions of the constituents of the material. The effective material properties are estimated using a simple power law based on rule of mixture. The accuracy of the presented results is verified through comparisons with available results in the published literature. Furthermore, parametric studies are performed to examine the influences of the power of solar FGM, aspect ratio, foundation stiffness coefficients and thermal loading types on the critical buckling load of solar FGM rectangular plates.

2. Problem formulation

2.1 Physical neutral surface

Functionally graded materials are a special kind of composites in which their material properties vary smoothly and continuously due to gradually varying the volume fraction of the constituent materials along certain dimension (usually in the thickness direction). In this study, the FGM plate is made from a mixture of ceramic and metal and the properties are assumed to vary through the thickness of the plate. Due to asymmetry of material properties of FGM plates with respect to middle plane, the stretching and bending equations are coupled. But, if the origin of the coordinate system is suitably selected in the thickness direction of the FGM plate so as to be the neutral surface, the properties of the FGM plate being symmetric with respect to it. To specify the position of neutral surface of FGM plates, two different planes are considered for the measurement of z, namely, z_{ms} and z_{ns} measured from the middle surface and the neutral surface of the plate, respectively, as depicted in Fig. 1.

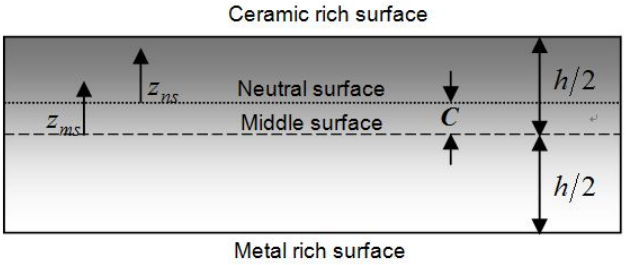

Fig. 1 The position of middle surface and neutral surface for a functionally graded plate

The volume-fraction of ceramic V_C is expressed based on z_{ms} and z_{ns} coordinates as

$$V_C = \left(\frac{z_{ms}}{h} + \frac{1}{2}\right)^k = \left(\frac{z_{ns} + C}{h} + \frac{1}{2}\right)^k \tag{1}$$

where k is the power law index which takes the value greater or equal to zero and C is the distance of neutral surface from the mid-surface. Material non-homogeneous properties of a functionally graded material plate may be obtained by means of the Voigt rule of mixture (Suresh and Mortensen 1998). Thus, using Eq. (1), the material non-homogeneous properties of FG plate P, as a function of thickness coordinate, become

$$P(z) = P_M + P_{CM}\left(\frac{z_{ns} + C}{h} + \frac{1}{2}\right)^k, \quad P_{CM} = P_C - P_M \tag{2}$$

where P_M and P_C are the corresponding properties of the metal and ceramic, respectively. In the present work, we assume that the elasticity modules E, and the thermal expansion coefficient α, are described by Eq. (2), while Poisson's ratio v, is considered to be constant across the thickness. The position of the neutral surface of the FG plate is determined to satisfy the first moment with respect to Young's modulus being zero as follows (Zhang and Zhou 2008, Bourada *et al*. 2015, Meradjah *et al*. 2015, Al-Basyouni *et al*. 2015)

$$\int_{-h/2}^{h/2} E(z_{ms})(z_{ms} - C)dz_{ms} = 0 \tag{3}$$

Consequently, the position of neutral surface can be obtained as

$$C = \frac{\int_{-h/2}^{h/2} E(z_{ms}) z_{ms} dz_{ms}}{\int_{-h/2}^{h/2} E(z_{ms}) dz_{ms}} \tag{4}$$

It is clear that the parameter C is zero for homogeneous isotropic plates, as expected.

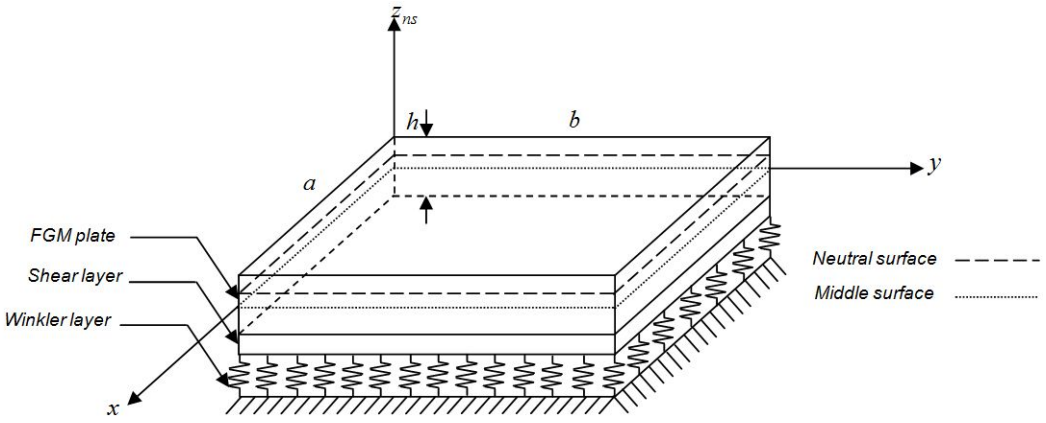

Fig. 2 Coordinate system and geometry for rectangular FG plates on elastic foundation

2.2 Theoretical model

Consider a rectangular FGM plate with the length a, width b and uniform thickness h, resting on two-parameter elastic foundation is considered as depicted in Fig. 2. Unlike the other shear deformation theory, just four unknowns functions are needed in the proposed efficient hyperbolic shear deformation theory.

2.2.1 Basic assumptions

Assumptions of the present theory are as follows:

(i) The origin of the Cartesian coordinate system is taken at the neutral surface of the FGM plate.

(ii) The transverse displacement w includes two components of bending w_b, and shear w_s. These components are functions of coordinates x, y only

$$w(x, y, z_{ns}) = w_b(x, y) + w_s(x, y) \tag{5}$$

(iii) The transverse normal stress σ_z is negligible in comparison with in-plane stresses σ_x and σ_y.

(iv) The displacements u in x-direction and v in y-direction consist of extension, bending, and shear components

$$u = u_0 + u_b + u_s, \qquad v = v_0 + v_b + v_s \tag{6}$$

The bending components u_b and v_b are assumed to be similar to the displacements given by the classical plate theory. Therefore, the expression for u_b and v_b can be given as

$$u_b = -z_{ns}\frac{\partial w_b}{\partial x}, \qquad v_b = -z_{ns}\frac{\partial w_b}{\partial y} \tag{7}$$

The shear components u_s and v_s give rise, in conjunction with w_s, to the parabolic variations of shear strains γ_{xz}, γ_{yz} and hence to shear stresses τ_{xz}, τ_{yz} through the thickness of the plate in such a way that shear stresses τ_{xz}, τ_{yz} are zero at the top and bottom faces of the plate. Consequently, the expression for u_s and v_s can be given as

$$u_s = -f(z_{ns})\frac{\partial w_s}{\partial x}, \qquad v_s = -f(z_{ns})\frac{\partial w_s}{\partial y} \tag{8}$$

It is noted that in this work the shape function $f(z_{ns})$ developed by Hebali *et al*. (2014) is modified based on the concept of the neutral surface position as follows

$$f(z_{ns}) = \frac{(h/\pi)\sinh\left(\frac{\pi}{h}(z_{ns}+C)\right) - (z_{ns}+C)}{\left[\cosh(\pi/2) - 1\right]} \tag{9}$$

2.2.2 Kinematics

Based on the assumptions made in the preceding section, the displacement field can be obtained using Eqs. (5)-(9) as

$$u(x,y,z_{ns}) = u_0(x,y) - z_{ns}\frac{\partial w_b}{\partial x} - f(z_{ns})\frac{\partial w_s}{\partial x} \tag{10a}$$

$$v(x,y,z_{ns}) = v_0(x,y) - z_{ns}\frac{\partial w_b}{\partial y} - f(z_{ns})\frac{\partial w_s}{\partial y} \tag{10b}$$

$$w(x,y,z_{ns}) = w_b(x,y) + w_s(x,y) \tag{10c}$$

The non-linear von Karman strain–displacement equations are as follows

$$\begin{Bmatrix}\varepsilon_x\\ \varepsilon_y\\ \gamma_{xy}\end{Bmatrix} = \begin{Bmatrix}\varepsilon_x^0\\ \varepsilon_y^0\\ \gamma_{xy}^0\end{Bmatrix} + z_{ns}\begin{Bmatrix}k_x^b\\ k_y^b\\ k_{xy}^b\end{Bmatrix} + f(z_{ns})\begin{Bmatrix}k_x^s\\ k_y^s\\ k_{xy}^s\end{Bmatrix}, \qquad \begin{Bmatrix}\gamma_{yz}\\ \gamma_{xz}\end{Bmatrix} = g(z_{ns})\begin{Bmatrix}\gamma_{yz}^s\\ \gamma_{xz}^s\end{Bmatrix} \tag{11}$$

where

$$\begin{Bmatrix}\varepsilon_x^0\\ \varepsilon_y^0\\ \gamma_{xy}^0\end{Bmatrix} = \begin{Bmatrix}\dfrac{\partial u_0}{\partial x} + \dfrac{1}{2}\left(\dfrac{\partial w_b}{\partial x} + \dfrac{\partial w_s}{\partial x}\right)^2\\ \dfrac{\partial v_0}{\partial x} + \dfrac{1}{2}\left(\dfrac{\partial w_b}{\partial y} + \dfrac{\partial w_s}{\partial y}\right)^2\\ \dfrac{\partial u_0}{\partial y} + \dfrac{\partial v_0}{\partial x} + \left(\dfrac{\partial w_b}{\partial x} + \dfrac{\partial w_s}{\partial x}\right)\left(\dfrac{\partial w_b}{\partial y} + \dfrac{\partial w_s}{\partial y}\right)\end{Bmatrix},$$

$$\begin{Bmatrix}k_x^b\\ k_y^b\\ k_{xy}^b\end{Bmatrix} = \begin{Bmatrix}-\dfrac{\partial^2 w_b}{\partial x^2}\\ -\dfrac{\partial^2 w_b}{\partial y^2}\\ -2\dfrac{\partial^2 w_b}{\partial x \partial y}\end{Bmatrix}, \qquad \begin{Bmatrix}k_x^s\\ k_y^s\\ k_{xy}^s\end{Bmatrix} = \begin{Bmatrix}-\dfrac{\partial^2 w_s}{\partial x^2}\\ -\dfrac{\partial^2 w_s}{\partial y^2}\\ -2\dfrac{\partial^2 w_s}{\partial x \partial y}\end{Bmatrix}, \qquad \begin{Bmatrix}\gamma_{yz}^s\\ \gamma_{xz}^s\end{Bmatrix} = \begin{Bmatrix}\dfrac{\partial w_s}{\partial y}\\ \dfrac{\partial w_s}{\partial x}\end{Bmatrix} \tag{12a}$$

and

$$g(z_{ns}) = 1 - \frac{df(z_{ns})}{dz_{ns}} \tag{12b}$$

2.2.3 Constitutive relations

The plate is subjected to a thermal load $T(x, y, z_{ns})$. The linear constitutive relations are

$$\begin{Bmatrix} \sigma_x \\ \sigma_y \\ \tau_{xy} \end{Bmatrix} = \begin{bmatrix} Q_{11} & Q_{12} & 0 \\ Q_{12} & Q_{22} & 0 \\ 0 & 0 & Q_{66} \end{bmatrix} \begin{Bmatrix} \varepsilon_x - \alpha T \\ \varepsilon_y - \alpha T \\ \gamma_{xy} \end{Bmatrix} \quad \text{and} \quad \begin{Bmatrix} \tau_{yz} \\ \tau_{zx} \end{Bmatrix} = \begin{bmatrix} Q_{44} & 0 \\ 0 & Q_{55} \end{bmatrix} \begin{Bmatrix} \gamma_{yz} \\ \gamma_{zx} \end{Bmatrix} \tag{13}$$

where (σ_x, σ_y, τ_{xy}, τ_{yz}, τ_{yx}) and (ε_x, ε_y, γ_{xy}, γ_{yz}, γ_{yx}) are the stress and strain components, respectively. Using the material properties defined in Eq. (2), stiffness coefficients, Q_{ij}, can be expressed as

$$Q_{11} = Q_{22} = \frac{E(z_{ns})}{1-\nu^2}, \tag{14a}$$

$$Q_{12} = \frac{\nu\, E(z_{ns})}{1-\nu^2}, \tag{14b}$$

$$Q_{44} = Q_{55} = Q_{66} = \frac{E(z_{ns})}{2(1+\nu)}, \tag{14c}$$

2.2.4 Stability equations

The equilibrium equations of the FG plate resting on the Pasternak elastic foundation under thermal loadings may be derived on the basis of the stationary potential energy. The total potential energy of the plate, V, may be written in the form

$$V = U + U_F \tag{15}$$

Here, U is the total strain energy of the plate, and is calculated as (Zenkour and Sobhy 2010 and 2011)

$$U = \frac{1}{2}\int_0^a \int_0^b \int_{-\frac{h}{2}-C}^{\frac{h}{2}-C} \left[\sigma_x\left(\varepsilon_x - \alpha T\right) + \sigma_y\left(\varepsilon_y - \alpha T\right) + \tau_{xy}\gamma_{xy} + \tau_{yz}\gamma_{yz} + \tau_{xz}\gamma_{xz}\right] dz_{ns}\, dy dx, \tag{16}$$

and U_F is the strain energy due to the Pasternak elastic foundation, which is given by (Ait Atmane *et al*. 2010)

$$U_F = \frac{1}{2}\int_0^a \int_0^b f_e(w_b + w_s)\, dy dx \tag{17}$$

where f_e is the density of reaction force of foundation. For the Pasternak foundation model (Zenkour 2009, Zenkour *et al*. 2014, Besseghier *et al*. 2015)

$$f_e = K_W(w_b + w_s) - K_g\nabla^2(w_b + w_s) \tag{18}$$

where K_W is the Winkler foundation stiffness and K_g is a constant showing the effect of the shear interactions of the vertical elements.

Using Eqs. (11), (12) and (13) and employing the virtual work principle to minimize the functional of total potential energy function result in the expressions for the equilibrium equations of plate resting on two parameters elastic foundation as

$$\begin{aligned}
&\frac{\partial N_x}{\partial x} + \frac{\partial N_{xy}}{\partial y} = 0\\
&\frac{\partial N_{xy}}{\partial x} + \frac{\partial N_y}{\partial y} = 0\\
&\frac{\partial^2 M_x^b}{\partial x^2} + 2\frac{\partial^2 M_{xy}^b}{\partial x\partial y} + \frac{\partial^2 M_y^b}{\partial y^2} + \overline{N} - f_e = 0\\
&\frac{\partial^2 M_x^s}{\partial x^2} + 2\frac{\partial^2 M_{xy}^s}{\partial x\partial y} + \frac{\partial^2 M_y^s}{\partial y^2} + \frac{\partial S_{xz}^s}{\partial x} + \frac{\partial S_{yz}^s}{\partial y} + \overline{N} - f_e = 0
\end{aligned} \tag{19}$$

with

$$\overline{N} = \left[N_x \frac{\partial^2(w_b + w_s)}{\partial x^2} + 2N_{xy}\frac{\partial^2(w_b + w_s)}{\partial x\partial y} + N_y\frac{\partial^2(w_b + w_s)}{\partial y^2} \right] \tag{20}$$

and

$$\begin{Bmatrix} N_x, & N_y, & N_{xy} \\ M_x^b, & M_y^b, & M_{xy}^b \\ M_x^s, & M_y^s, & M_{xy}^s \end{Bmatrix} = \int_{-h/2-C}^{h/2-C} (\sigma_x, \sigma_y, \tau_{xy}) \begin{Bmatrix} 1 \\ z_{ns} \\ f(z_{ns}) \end{Bmatrix} dz_{ns}, \tag{21a}$$

$$(S_{xz}^s, S_{yz}^s) = \int_{-h/2-C}^{h/2-C} (\tau_{xz}, \tau_{yz}) g(z_{ns}) dz_{ns}. \tag{21b}$$

Using Eq. (13) in Eq. (21), the stress resultants of the FGM plate can be related to the total strains by

$$\begin{Bmatrix} N \\ M^b \\ M^s \end{Bmatrix} = \begin{bmatrix} A & 0 & B^s \\ 0 & D & D^s \\ B^s & D^s & H^s \end{bmatrix} \begin{Bmatrix} \varepsilon \\ k^b \\ k^s \end{Bmatrix} - \begin{Bmatrix} N^T \\ M^{bT} \\ M^{sT} \end{Bmatrix}, \qquad S = A^s\gamma, \tag{22}$$

where

$$N = \{N_x, N_y, N_{xy}\}^t, \qquad M^b = \{M_x^b, M_y^b, M_{xy}^b\}^t, \qquad M^s = \{M_x^s, M_y^s, M_{xy}^s\}^t, \tag{23a}$$

$$N^T = \{N_x^T, N_y^T, 0\}^t, \qquad M^{bT} = \{M_x^{bT}, M_y^{bT}, 0\}^t, \qquad M^{sT} = \{M_x^{sT}, M_y^{sT}, 0\}^t, \tag{23b}$$

$$\varepsilon = \left\{\varepsilon_x^0, \varepsilon_y^0, \gamma_{xy}^0\right\}^t, \qquad k^b = \left\{k_x^b, k_y^b, k_{xy}^b\right\}^t, \qquad k^s = \left\{k_x^s, k_y^s, k_{xy}^s\right\}^t, \tag{23c}$$

$$A = \begin{bmatrix} A_{11} & A_{12} & 0 \\ A_{12} & A_{22} & 0 \\ 0 & 0 & A_{66} \end{bmatrix}, \qquad D = \begin{bmatrix} D_{11} & D_{12} & 0 \\ D_{12} & D_{22} & 0 \\ 0 & 0 & D_{66} \end{bmatrix}, \tag{23d}$$

$$B^s = \begin{bmatrix} B_{11}^s & B_{12}^s & 0 \\ B_{12}^s & B_{22}^s & 0 \\ 0 & 0 & B_{66}^s \end{bmatrix}, \qquad D^s = \begin{bmatrix} D_{11}^s & D_{12}^s & 0 \\ D_{12}^s & D_{22}^s & 0 \\ 0 & 0 & D_{66}^s \end{bmatrix}, \qquad H^s = \begin{bmatrix} H_{11}^s & H_{12}^s & 0 \\ H_{12}^s & H_{22}^s & 0 \\ 0 & 0 & H_{66}^s \end{bmatrix}, \tag{23e}$$

$$S = \left\{S_{yz}^s, S_{xz}^s\right\}^t, \qquad \gamma = \left\{\gamma_{yz}, \gamma_{xz}\right\}^t, \qquad A^s = \begin{bmatrix} A_{44}^s & 0 \\ 0 & A_{55}^s \end{bmatrix}, \tag{23f}$$

where A_{ij}, D_{ij}, etc., are the plate stiffness, defined by

$$\begin{Bmatrix} A_{11} & D_{11} & B_{11}^s & D_{11}^s & H_{11}^s \\ A_{12} & D_{12} & B_{12}^s & D_{12}^s & H_{12}^s \\ A_{66} & D_{66} & B_{66}^s & D_{66}^s & H_{66}^s \end{Bmatrix} = \int_{-\frac{h}{2}-C}^{\frac{h}{2}-C} Q_{11}\left(1, z^2, f(z_{ns}), z_{ns}\, f(z_{ns}), f^2(z_{ns})\right) \begin{Bmatrix} 1 \\ \nu \\ \dfrac{1-\nu}{2} \end{Bmatrix} dz_{ns}, \tag{24a}$$

and

$$\left(A_{22}, D_{22}, B_{22}^s, D_{22}^s, H_{22}^s\right) = \left(A_{11}, D_{11}, B_{11}^s, D_{11}^s, H_{11}^s\right), \tag{24b}$$

$$A_{44}^s = A_{55}^s = \int_{-\frac{h}{2}-C}^{\frac{h}{2}-C} \frac{E(z_{ns})}{2(1+\nu)} \left[g(z_{ns})\right]^2 dz_{ns}, \tag{24c}$$

The stress and moment resultants, $N_x^T = N_y^T$, $M_x^{bT} = M_y^{bT}$, and $M_x^{sT} = M_y^{sT}$ due to thermal loading are defined by

$$\begin{Bmatrix} N_x^T \\ M_x^{bT} \\ M_x^{sT} \end{Bmatrix} = \int_{-\frac{h}{2}-C}^{\frac{h}{2}-C} \frac{E(z_{ns})}{1-\nu} \alpha(z_{ns}) T \begin{Bmatrix} 1 \\ z \\ f(z_{ns}) \end{Bmatrix} dz_{ns}, \tag{25}$$

The stability equations for FGM plates may be obtained by mean of the adjacent-equilibrium criterion. Let us assume that the state of equilibrium of sandwich plate under thermal loads is defined in terms of the displacement components u_0^0, v_0^0, w_b^0 and w_s^0. The displacement components of a neighbouring state of the stable equilibrium differ by u_0^1, v_0^1, w_b^1, w_s^1 with respect to the equilibrium position. Thus, the total displacements of a neighbouring state are

$$u_0 = u_0^0 + u_0^1, \qquad v_0 = v_0^0 + v_0^1, \qquad w_b = w_b^0 + w_b^1, \qquad w_s = w_s^0 + w_s^1 \tag{26}$$

Accordingly, the stress resultants are divided into two terms representing the stable equilibrium and the neighbouring state. The stress resultants with superscript 1 are linear functions of displacement with superscript 1. Considering all these mentioned above and using Eqs. (19) and (26), the stability equations becomes

$$\begin{aligned}
&\frac{\partial N_x^1}{\partial x}+\frac{\partial N_{xy}^1}{\partial y}=0\\
&\frac{\partial N_{xy}^1}{\partial x}+\frac{\partial N_y^1}{\partial y}=0\\
&\frac{\partial^2 M_x^{b1}}{\partial x^2}+2\frac{\partial^2 M_{xy}^{b1}}{\partial x\partial y}+\frac{\partial^2 M_y^{b1}}{\partial y^2}+\overline{N}^1-f_e^1=0\\
&\frac{\partial^2 M_x^{s1}}{\partial x^2}+2\frac{\partial^2 M_{xy}^{s1}}{\partial x\partial y}+\frac{\partial^2 M_y^{s1}}{\partial y^2}+\frac{\partial S_{xz}^{s1}}{\partial x}+\frac{\partial S_{yz}^{s1}}{\partial y}+\overline{N}^1-f_e^1=0
\end{aligned} \tag{27}$$

with

$$\overline{N}^1=\left[N_x^0\frac{\partial^2\left(w_b^1+w_s^1\right)}{\partial x^2}+2N_{xy}^0\frac{\partial^2\left(w_b^1+w_s^1\right)}{\partial x\partial y}+N_y^0\frac{\partial^2\left(w_b^1+w_s^1\right)}{\partial y^2}\right] \tag{28a}$$

$$f_e^1=K_W(w_b^1+w_s^1)-K_g\nabla^2(w_b^1+w_s^1) \tag{28b}$$

The terms N_x^0, N_y^0 and N_{xy}^0 are the pre-buckling force resultants obtained as

$$N_x^0=N_y^0=-\int_{-h/2-C}^{h/2-C}\frac{\alpha(z_{ns})E(z_{ns})T}{1-\nu}dz_{ns}\,,\qquad N_{xy}^0=0 \tag{29}$$

2.3 Trigonometric solution to thermal buckling

Rectangular plates are generally classified in accordance with the type of support used. We are here concerned with the exact solution of Eq. (27) for a simply supported FGM plate. The following boundary conditions are imposed for the present refined shear deformation theory at the side edges

$$v_0^1=w_b^1=w_s^1=\frac{\partial w_s^1}{\partial y}=N_x^1=M_x^{b1}=M_x^{s1}=0\qquad\text{at}\qquad x=0,\ a, \tag{30a}$$

$$u_0^1=w_b^1=w_s^1=\frac{\partial w_s^1}{\partial x}=N_y^1=M_y^{b1}=M_y^{s1}=0\qquad\text{at}\qquad y=0,\ b. \tag{30b}$$

The following approximate solution is seen to satisfy both the differential equation and the boundary conditions

$$\begin{Bmatrix} u_0^1 \\ v_0^1 \\ w_b^1 \\ w_s^1 \end{Bmatrix} = \sum_{m=1}^{\infty}\sum_{n=1}^{\infty} \begin{Bmatrix} U_{mn}^1 \cos(\lambda x)\sin(\mu y) \\ V_{mn}^1 \sin(\lambda x)\cos(\mu y) \\ W_{bmn}^1 \sin(\lambda x)\sin(\mu y) \\ W_{smn}^1 \sin(\lambda x)\sin(\mu y) \end{Bmatrix} \tag{31}$$

where $U_{mn}^1, V_{mn}^1, W_{bmn}^1,$ and W_{smn}^1 are arbitrary parameters to be determined and $\lambda = m\pi / a$ and $\mu = n\pi / b.$ Substituting Eqs. (22) and (31) into Eq. (27), one obtains

$$[K]\{\Delta\} = 0, \tag{32}$$

where $\{\Delta\}$ denotes the column

$$\{\Delta\} = \left\{U_{mn}^1, V_{mn}^1, W_{bmn}^1, W_{smn}^1\right\}^t \tag{33}$$

and [*K*] is the symmetric matrix given by

$$[K] = \begin{bmatrix} a_{11} & a_{12} & a_{13} & a_{14} \\ a_{12} & a_{22} & a_{23} & a_{24} \\ a_{13} & a_{23} & a_{33} & a_{34} \\ a_{14} & a_{24} & a_{34} & a_{44} \end{bmatrix}, \tag{34}$$

in which

$$\begin{aligned}
a_{11} &= -\left(A_{11}\lambda^2 + A_{66}\mu^2\right) \\
a_{12} &= -\lambda\,\mu\left(A_{12} + A_{66}\right) \\
a_{13} &= 0 \\
a_{14} &= \lambda\left[B_{11}^s\lambda^2 + (B_{12}^s + 2B_{66}^s)\,\mu^2\right] \\
a_{22} &= -\left(A_{66}\lambda^2 + A_{22}\mu^2\right) \\
a_{23} &= 0 \\
a_{24} &= \mu\left[(B_{12}^s + 2B_{66}^s)\,\lambda^2 + B_{22}^s\mu^2\right] \\
a_{33} &= -\left(D_{11}\lambda^4 + 2(D_{12} + 2D_{66})\lambda^2\mu^2 + D_{22}\mu^4 + N_x^0\lambda^2 + N_y^0\mu^2 + K_g\left(\lambda^2 + \mu^2\right) + K_W\right) \\
a_{34} &= -\left(D_{11}^s\lambda^4 + 2(D_{12}^s + 2D_{66}^s)\lambda^2\,\mu^2 + D_{22}^s\,\mu^4 + N_x^0\lambda^2 + N_y^0\mu^2 + K_g\left(\lambda^2 + \mu^2\right) + K_W\right) \\
a_{44} &= -\begin{pmatrix} H_{11}^s\lambda^4 + 2(H_{12}^s + 2H_{66}^s)\lambda^2\mu^2 + H_{22}^s\mu^4 + A_{55}^s\lambda^2 + A_{44}^s\mu^2 \\ + N_x^0\lambda^2 + N_y^0\mu^2 + K_g\left(\lambda^2 + \mu^2\right) + K_W \end{pmatrix}
\end{aligned} \tag{35}$$

and [*K*] is the symmetric matrix given by

$$\begin{bmatrix} [K^{11}] & [K^{12}] \\ [K^{12}]^T & [K^{22}] \end{bmatrix} \begin{Bmatrix} \Delta^1 \\ \Delta^2 \end{Bmatrix} = \begin{Bmatrix} 0 \\ 0 \end{Bmatrix} \tag{36}$$

where

$$\left[K^{11}\right]=\begin{bmatrix} a_{11} & a_{12} \\ a_{12} & a_{22} \end{bmatrix}, \quad \left[K^{12}\right]=\begin{bmatrix} 0 & a_{14} \\ 0 & a_{24} \end{bmatrix}, \quad \left[K^{22}\right]=\begin{bmatrix} a_{33} & a_{34} \\ a_{34} & a_{44} \end{bmatrix} \tag{37a}$$

$$\Delta^1=\begin{Bmatrix} U^1_{mn} \\ V^1_{mn} \end{Bmatrix}, \quad \Delta^2=\begin{Bmatrix} W^1_{bmn} \\ W^1_{smn} \end{Bmatrix} \tag{37b}$$

Eq. (37) represents a pair of two matrix equations

$$\left[K^{11}\right]\Delta^1+\left[K^{12}\right]\Delta^2=0 \tag{38a}$$

$$\left[K^{12}\right]^T\Delta^1+\left[K^{22}\right]\Delta^2=0 \tag{38a}$$

Solving Eq. (39a) for Δ^1 and then substituting the result into Eq. (39b), the following equation is obtained

$$\left[\overline{K}^{22}\right]\Delta^2=0 \tag{39}$$

where

$$\left[\overline{K}^{22}\right]=\left[K^{22}\right]-\left[K^{12}\right]^T\left[K^{11}\right]^{-1}\left[K^{12}\right]=\begin{bmatrix} a_{33} & a_{34} \\ a_{34} & b_{44} \end{bmatrix} \tag{40a}$$

and

$$\begin{gathered} \overline{a}_{33}=a_{33}, \quad \overline{a}_{34}=a_{34}, \quad \overline{a}_{43}=a_{34}, \quad b_{44}=a_{44}-a_{14}\frac{b_1}{b_0}-a_{24}\frac{b_2}{b_0}, \\ b_0=a_{11}a_{22}-a_{12}^2, \quad b_1=a_{14}a_{22}-a_{12}a_{24}, \quad b_2=a_{11}a_{24}-a_{12}a_{14} \end{gathered} \tag{40b}$$

For nontrivial solution, the determinant of the coefficient matrix in Eq. (40) must be zero. This gives the following expression for the thermal buckling load

$$N_x^0=N_y^0=\frac{1}{\lambda^2+\mu^2}\frac{a_{33}b_{44}-a_{34}^2}{a_{33}+a_{44}-2a_{34}} \tag{41}$$

2.3.1 Buckling of FG plates under uniform temperature rise

The plate initial temperature is assumed to be T_i. The temperature is uniformly raised to a final value T_f in which the plate buckles. The temperature change is $\Delta T = T_f - T_i$. Using this distribution of temperature, the critical buckling temperature change ΔT_{cr} becomes by using Eqs. (29) and (42)

$$\Delta T_{cr}=\frac{1}{\overline{\beta}_1\left(\lambda^2+\mu^2\right)}\frac{a_{33}b_{44}-a_{34}^2}{a_{33}+a_{44}-2a_{34}} \tag{42a}$$

where

$$\overline{\beta}_1 = -\int_{-h/2-C}^{h/2-C} \frac{\alpha(z_{ns})E(z_{ns})}{1-\nu} dz_{ns}. \tag{42b}$$

2.3.2 Buckling of FG plates subjected to graded temperature change across the thickness

We assume that the temperature of the top surface is T_M and the temperature varies from T_M, according to the power law variation through-the-thickness, to the bottom surface temperature T_M in which the plate buckles. In this case, the temperature through-the-thickness proposed by (Zenkour and Sobhy 2010 and 2011) is modified by considering the concept of physical neutral surface

$$T(z_{ns}) = \Delta T\left(\frac{z_{ns}+C}{h}+\frac{1}{2}\right)^{\gamma} + T_M, \tag{43}$$

where the buckling temperature difference $\Delta T = T_C - T_M$ and γ is the temperature exponent ($0 < \gamma < \infty$). Note that the value of γ equal to unity represents a linear temperature change across the thickness. While the value of γ excluding unity represents a non-linear temperature change through-the-thickness.

Similar to the previous loading case, the critical buckling temperature change ΔT_{cr} becomes by using Eqs. (29) and (42)

$$\Delta T_{cr} = \frac{a_{33}b_{44} - a_{34}^2 + T_M\overline{\beta}_1\left(\lambda^2+\mu^2\right)\left(a_{33}+a_{44}-2a_{34}\right)}{\overline{\beta}_2(\lambda^2+\mu^2)(a_{33}+a_{44}-2a_{34})} \tag{44a}$$

where

$$\overline{\beta}_2 = -\int_{-h/2-C}^{h/2-C} \frac{\alpha(z_{ns})E(z_{ns})}{1-\nu}\left(\frac{z_{ns}+C}{h}+\frac{1}{2}\right)^{\gamma} dz_{ns} \tag{44b}$$

Note that the value of γ equal to unity represents a linear temperature change across the thickness. While the value of γ excluding unity represents a non-linear temperature change through the thickness.

3. Numerical results and discussion

The general approach outlined in the previous sections for the thermal buckling analysis of the homogeneous and solar FG plates under uniform, linear and non-linear temperature rises through the thickness is illustrated in this section using the present efficient hyperbolic plate theory based on exact neutral surface position. The solar FG plate is taken to be made of Aluminum and Alumina with the following material properties:

- Metal (Aluminium, Al): $E_M = 70$ GPa; $\nu = 0.3$; $\alpha_M = 23.\ 10^{-6}$/°C; $k_M = 204$ W/mL.
- Ceramic (Alumina, Al_2O_3): $E_C = 380$ GPa; $\nu = 0.3$; $\alpha_C = 7.4\ 10^{-6}$/°C; $k_C = 10.4$ W/mK.

For the non-linear temperature rises through the thickness, the temperature rises 5°C in the metal-rich surface of the plate (i.e., $T_m = 5$°C). The shear correction factor of FPT is fixed to be 5/6.

The following dimensionless of Winkler's and Pasternak's elastic foundation parameters, as well as the critical buckling temperature difference are used in the present analysis

$$k_w = \frac{a^4}{D} K_W, \quad k_g = \frac{a^2}{D} K_g, \quad T_{cr} = 10^{-3} \Delta T_{cr} \tag{45}$$

where $D = E_C h^3 / [12(1-\nu^2)]$.

3.1 Comparative studies

In order to demonstrate the accuracy of the present closed-form exact solution, the correlation between the present theory and different higher- and first-order shear deformation theories and classical plate theory is established. The description of various displacement models is given in Table 1.

Results were obtained for foundationless FG plates (k = 1) under uniform temperature rise through the thickness based on the present theory with only four unknown functions and compared with those other various theories (Samsam Shariat and Eslami 2007, Lanhe 2004, Zenkour and Sobhy 2011) with five unknown functions as shown in Table 2. It is observed that the obtained

Table 1 Displacement models

Model	Theory	Unknown functions
CPT	Classical plate theory	3
FPT	First-order shear deformation theory (Zenkour and Sobhy 2011)	5
TPT	Trigonometric shear deformation plate theory (Zenkour and Sobhy 2011)	5
HPT	Higher order shear deformation theory (Zenkour and Sobhy 2011, Reddy 2000)	5
Present	Present hyperbolic plate theory	4

Table 2 Critical buckling temperature change T_{cr} of foundationless FG plates under uniform temperature rise versus the side-to-thickness and aspect ratios based on the various theories

a/*b*	Theory	*a* / *h* = 10	*a* / *h* = 20	*a* / *h* = 40	*a* / *h* = 60	*a* / *h* = 80	*a* / *h* = 100
1	Present	0.758423	0.196267	0.049501	0.022037	0.0124029	0.0079400
	TPT[(a)]	0.758451	0.196269	0.049502	0.022037	0.012403	0.007940
	HPT[(a)]	0.758396	0.196265	0.049502	0.022037	0.012403	0.007940
	CPT[(a)]	0.794377	0.198594	0.049649	0.022066	0.012412	0.007944
2	Present	1.77567	0.482196	0.123208	0.054983	0.0309729	0.0198359
	TPT[(a)]	1.775899	0.482206	0.123209	0.054984	0.030973	0.019836
	HPT[(a)]	1.775555	0.482184	0.123208	0.054984	0.030973	0.019836
	HPT[(b)]	1.7756	0.48218	0.12321	0.05498	0.03097	0.01984
	FPT[(c)]	1.8072	0.48451	0.12336	0.05501	0.03098	0.01984
	CPT[(a)]	1.985943	0.496486	0.124121	0.055165	0.031030	0.019859

Table 2 Continued

a/*b*	Theory	*a* / *h* = 10	*a* / *h* = 20	*a* / *h* = 40	*a* / *h* = 60	*a* / *h* = 80	*a* / *h* = 100
3	Present	3.212203	0.937430	0.244617	0.109608	0.0618316	0.0396248
	TPT[(a)]	3.213338	0.937475	0.244620	0.109609	0.061838	0.039625
	HPT[(a)]	3.211975	0.937389	0.244614	0.109608	0.061831	0.039625
	CPT[(a)]	3.971886	0.992972	0.248243	0.110330	0.062061	0.039719
4	Present	4.81864	1.53365	0.411643	0.185484	0.1048428	0.0672509
	TPT[(a)]	4.822477	1.533805	0.411650	0.185485	0.104843	0.067251
	HPT[(a)]	4.818675	1.533556	0.411634	0.185482	0.104842	0.067251
	HPT[(b)]	4.8187	1.5336	0.41163	0.18548	0.10484	0.06725
	FPT[(c)]	5.0530	1.5571	0.41333	0.18583	0.10495	0.06730
	CPT[(a)]	6.752207	1.688052	0.422013	0.187561	0.105503	0.067522

[(a)] Results taken from Zenkour and Sobhy (2011)
[(b)] Results taken from Samsam Shariat and Eslami (2007)
[(c)] Results taken from Lanhe (2004)

results using the present theory are identical to those computed by the other theories (Samsam Shariat and Eslami 2007, Lanhe 2004, Zenkour and Sobhy 2011) which validate the high accuracy of the present formulations and procedure.

Another comparative study for evaluation of critical buckling temperatures between the presented theory based on exact neutral surface position and analytical solution developed by Zenkour and Sobhy (2011) based on TPT, FPT and CPT, is performed in Tables 3 to 6. Indeed, Tables 3 to 5 exhibit the critical buckling temperature difference T_{cr} of FG square plate without elastic foundation or resting on one- or two-parameter elastic foundations for different values of the power law index k and the side-to-thickness ratio a/h using the present various plate theories.

Table 3 Critical buckling temperature change T_{cr} of FG square plates under uniform temperature rise for different values of the power law index and side-to-thickness ratio

		$k_w = 0, k_g = 0$			$k_w = 10, k_g = 0$			$k_w = 0, k_g = 10$		
k	Theory	*a*/*h* = 5	10	20	*a*/*h* = 5	10	20	*a*/*h* = 5	10	20
0	TPT[(a)]	5.58556	1.61882	0.42154	5.76109	1.66270	0.43252	9.22610	2.52896	0.64908
	HPT[(a)]	5.58344	1.61868	0.42154	5.75899	1.66257	0.43251	9.22398	2.52882	0.64907
	FPT[(a)]	5.58069	1.61862	0.42153	5.75622	1.66251	0.43251	9.22123	2.52876	0.64907
	CPT[(a)]	6.83964	1.70991	0.42748	7.01519	1.75380	0.43845	10.48019	2.62005	0.65501
	Present	5.58393	1.61875	0.42154	5.75947	1.66263	0.43251	9.22448	2.52888	0.64907
1	TPT[(a)]	2.67241	0.75845	0.19627	2.83603	0.79935	0.20649	6.06558	1.60674	0.40834
	HPT[(a)]	2.67153	0.75840	0.19627	2.83515	0.79930	0.20649	6.06470	1.60669	0.40835
	FPT[(a)]	2.67039	0.75837	0.19626	2.83400	0.79930	0.20649	6.06356	1.60667	0.40834
	CPT[(a)]	3.17751	0.79438	0.19859	3.34112	0.83528	0.20882	6.57068	1.64267	0.41067
	Present	2.67173	0.758423	0.19626	2.83534	0.79932	0.20649	6.06491	1.60671	0.40834

Table 3 Continued

		$k_w = 0, k_g = 0$			$k_w = 10, k_g = 0$			$k_w = 0, k_g = 10$		
k	Theory	$a/h = 5$	10	20	$a/h = 5$	10	20	$a/h = 5$	10	20
5	TPT[(a)]	2.27131	0.67895	0.17851	2.49808	0.73564	0.19268	6.97440	1.85472	0.47245
	HPT[(a)]	2.27501	0.67931	0.17854	2.50179	0.73600	0.19271	6.97810	1.85508	0.47248
	FPT[(a)]	2.35948	0.68678	0.17905	2.58625	0.74348	0.19322	7.06257	1.86255	0.47229
	CPT[(a)]	2.90629	0.72657	0.18164	3.13305	0.78326	0.19582	7.60938	1.90234	0.47559
	Present	2.27935	0.679719	0.17856	2.50612	0.73641	0.19273	6.98244	1.85549	0.47250
10	TPT[(a)]	2.27551	0.69254	0.18313	2.53146	0.75653	0.19913	7.58356	2.01955	0.51489
	HPT[(a)]	2.27678	0.69269	0.18314	2.53273	0.75668	0.19914	7.58483	2.01970	0.51490
	FPT[(a)]	2.36822	0.70108	0.18373	2.62417	0.76507	0.19972	7.67626	2.02809	0.51548
	CPT[(a)]	2.98770	0.74693	0.18673	3.24365	0.81091	0.20273	8.29575	2.07394	0.51848
	Present	2.27936	0.69295	0.18316	2.53530	0.75694	0.19915	7.58740	2.01996	0.51491

[(a)] Results taken from Zenkour and Sobhy (2011)

Table 4 Critical buckling temperature change T_{cr} of FG square plates under linear temperature rise for different values of the power law index and side-to-thickness ratio

		$k_w = 0, k_g = 0$			$k_w = 10, k_g = 0$			$k_w = 0, k_g = 10$		
K	Theory	$a/h = 5$	10	20	$a/h = 5$	10	20	$a/h = 5$	10	20
0	TPT[(a)]	11.16112	3.22764	0.83309	11.51220	3.31541	0.85503	18.44220	5.04791	1.28816
	HPT[(a)]	11.15688	3.22736	0.83307	11.50796	3.31513	0.85501	18.43797	5.04764	1.28814
	FPT[(a)]	11.15138	3.22725	0.833306	11.50246	3.31502	0.85501	18.43246	5.04752	1.28814
	CPT[(a)]	13.66929	3.40982	0.84496	14.02036	3.49759	0.86690	20.95037	5.23009	1.30002
	Present	11.15787	3.22750	0.83308	11.5089	3.31527	0.85502	18.43896	5.04777	1.28814
1	TPT[(a)]	5.00264	1.41307	0.35872	5.30948	1.48978	0.37789	11.36642	3.00402	0.75645
	HPT[(a)]	5.00099	1.41297	0.35871	5.30784	1.48968	0.37789	11.36477	3.00391	0.75645
	FPT[(a)]	4.99885	1.41292	0.35871	5.30570	1.48964	0.37789	11.36263	3.00387	0.75645
	CPT[(a)]	5.94993	1.48045	0.36308	6.25678	1.55716	0.38226	12.31372	3.07140	0.76082
	Present	5.00137	1.41302	0.358715	5.30822	1.48973	0.37789	11.36515	3.00396	0.756451
5	TPT[(a)]	3.90098	1.6006	0.28966	4.29132	1.25765	0.32306	11.99637	3.18391	0.80462
	HPT[(a)]	3.90735	1.16069	0.29871	4.29770	1.25827	0.32310	12.00275	3.18453	0.80467
	FPT[(a)]	4.05274	1.17354	0.29959	4.44308	1.27113	0.32399	12.14816	3.19739	0.80555
	CPT[(a)]	4.99396	1.24204	0.30405	5.38430	1.33962	0.32845	13.08936	3.26588	0.81002
	Present	3.91482	1.16138	0.29875	4.30516	1.25897	0.32315	12.01022	3.18523	0.80471
10	TPT[(a)]	4.02350	1.21837	0.31566	4.47705	1.33176	0.34401	13.42969	3.56992	0.90355
	HPT[(a)]	4.02576	1.21864	0.31568	4.47930	1.33203	0.34403	13.43194	3.57019	0.90357
	FPT[(a)]	4.18778	1.23350	0.31672	4.64132	1.34688	0.34506	13.59396	3.58504	0.90460
	CPT[(a)]	5.28555	1.31474	0.32204	5.73910	1.42813	0.35039	14.691174	3.66629	0.90993
	Present	4.03031	1.21910	0.31571	4.48386	1.33249	0.34406	13.43650	3.57065	0.90360

[(a)] Results taken from Zenkour and Sobhy (2011)

Table 5 Critical buckling temperature change T_{cr} of FG square plates under non-linear temperature rise (γ =3) for different values of the power law index and side-to-thickness ratio

		$k_w = 0, k_g = 0$			$k_w = 10, k_g = 0$			$k_w = 0, k_g = 10$		
k	Theory	$a/h = 5$	10	20	$a/h = 5$	10	20	$a/h = 5$	10	20
0	TPT[(a)]	22.32223	6.45528	1.66618	23.02439	6.63082	1.71006	36.88440	10.09582	2.57631
	HPT[(a)]	22.31376	6.45473	1.66614	23.01592	6.63027	1.71003	36.87594	10.09527	2.57628
	FPT[(a)]	22.30276	6.45450	1.66614	23.00491	6.63003	1.71002	36.86493	10.09527	2.57627
	CPT[(a)]	27.33857	6.81964	1.68991	28.04073	6.99518	1.73380	41.90074	10.46019	2.60005
	Present	22.31575	6.45501	1.66616	23.01791	6.63055	1.71004	36.87792	10.09555	2.57629
1	TPT[(a)]	10.00817	2.82696	0.71764	10.62205	2.98043	0.75601	22.73943	6.00978	1.51334
	HPT[(a)]	10.00488	2.82676	0.71763	10.61875	2.98022	0.75600	22.73614	6.00957	1.51333
	FPT[(a)]	10.00060	2.82667	0.71763	10.61447	2.98014	0.75600	22.73185	6.00948	1.51333
	CPT[(a)]	11.90332	2.96176	0.72637	12.51719	3.11523	0.76474	24.63458	6.14457	1.52207
	Present	10.00565	2.82686	0.71763	10.61952	2.98033	0.75600	22.73691	6.00967	1.51334
5	TPT[(a)]	6.77655	2.01520	0.51882	7.45464	2.18472	0.56120	20.83942	5.53091	1.39775
	HPT[(a)]	6.78763	2.01628	0.51889	7.46571	2.18580	0.56127	20.85050	5.53199	1.39782
	FPT[(a)]	7.04019	2.03861	0.52043	7.71827	2.20813	0.56281	21.10305	5.55433	1.39936
	CPT[(a)]	8.67523	2.15759	0.52819	9.35331	2.32711	0.57057	22.73809	5.67331	1.40711
	Present	6.80061	2.01749	0.51897	7.47869	2.18701	0.56135	20.86347	5.53321	1.39790
10	TPT[(a)]	6.92562	2.09717	0.54335	7.70631	2.29235	0.59214	23.11642	6.14487	1.55531
	HPT[(a)]	6.92950	2.09763	0.54338	7.71019	2.29281	0.59218	23.12029	6.14533	1.55531
	FPT[(a)]	7.20839	2.12321	0.54516	7.98908	2.31838	0.59396	23.39918	6.17091	1.55709
	CPT[(a)]	9.09798	2.26306	0.55433	9.87867	2.45823	0.60312	25.28877	6.31075	1.56625
	Present	6.93735	2.09843	0.54344	7.71804	2.29360	0.59223	23.12814	6.14613	1.55536

[(a)] Results taken from Zenkour and Sobhy (2011)

From the results presented in Tables 3 to 5, it is observed that results have a good agreement. Also, note that the results of critical buckling using the present theory are very close to those of HPT (Zenkour and Sobhy 2011). It is clear that the results have significant differences between the shear deformation plate theories and the classical plate one, indicating the shear deformation effect.

Finally, the present comparative studies show that the results obtained from the proposed method agree well with existing analytical results in the literature which validate the reliability and accuracy of the present analytical approach. It should be noted that the proposed efficient hyperbolic plate theory based on exact neutral surface position involves four unknowns as against five in case of other shear deformations theories TPT, HPT and FPT.

3.2 Parametric studies

In this section, to examine the effects of different parameters of plate and elastic foundation on the critical buckling temperature a solar FG plate, the comprehensive results are plotted in Figs. 3 to 9.

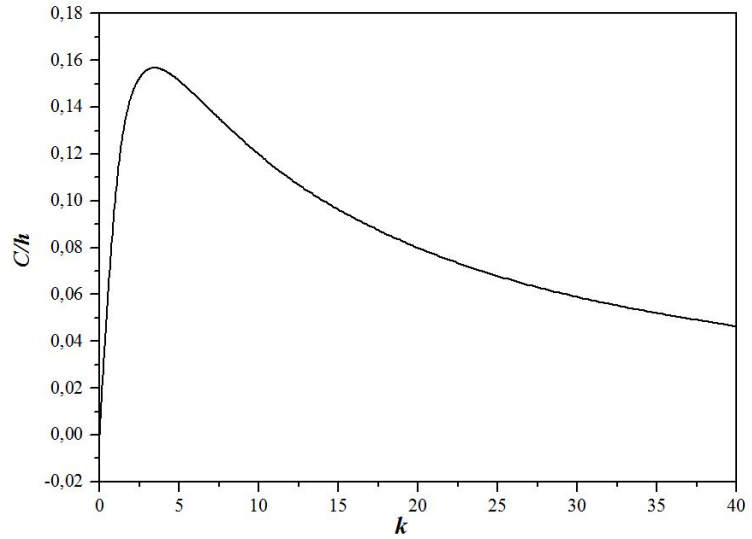

Fig. 3 Variation of the neutral surface position versus power law index

3.2.1 Effect of the power law index on location of the neutral surface

In order to better understand the location of the neutral surface, the variation of non-dimensional parameter C/h is depicted in Fig. 3 versus the power law index k of FGM. It can be observed when the power law index of FGM becomes zero (fully ceramic) or infinity (fully metallic); the neutral surface coincides on the middle surface, as expected.

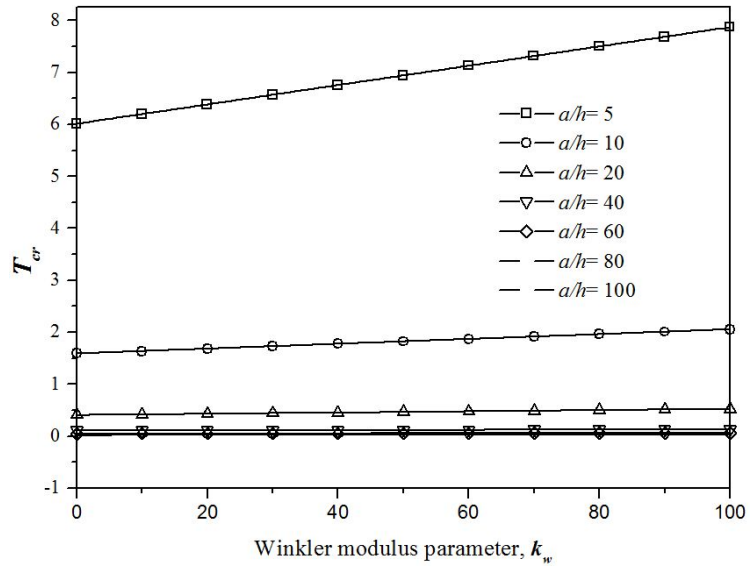

Fig. 4 Effect of Winkler modulus parameter on the critical buckling temperature of square FG plate for various side-to-thickness ratios a/h with $k_g = 10$ and $k = 2$.
(a) Uniform temperature; (b) Linear temperature; (c) Non-linear temperature $\gamma = 3$

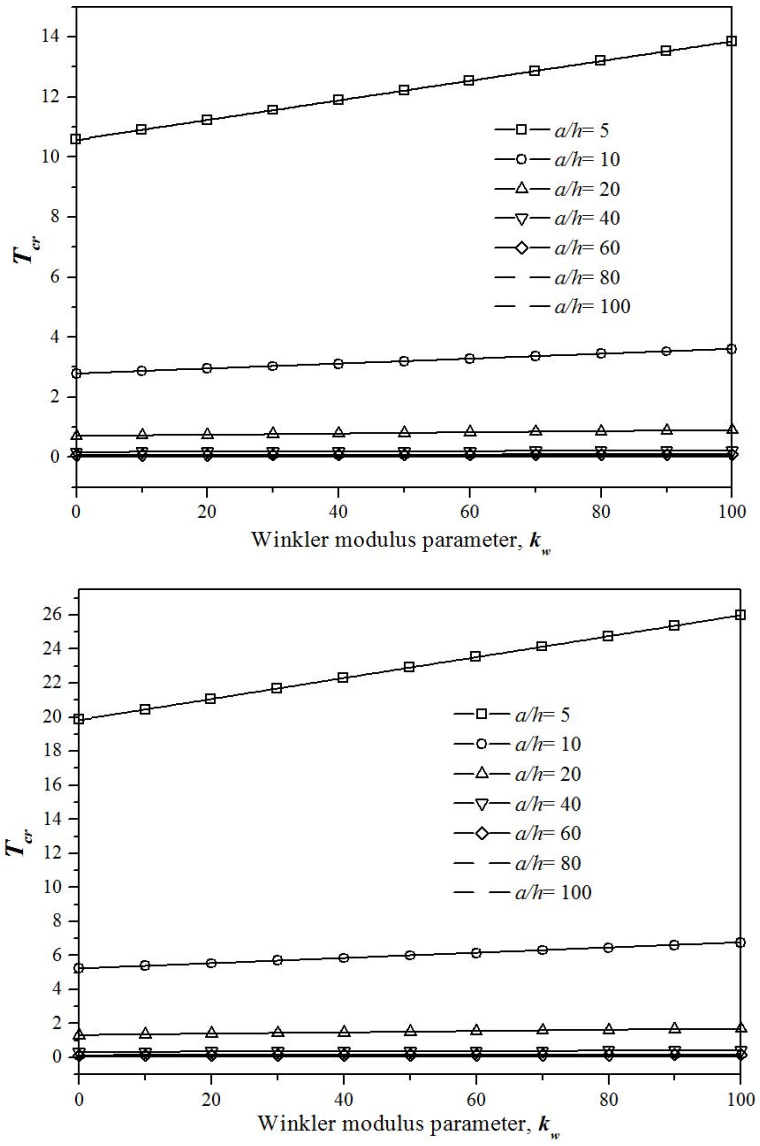

Fig. 4 Continued

3.2.2 Effect of Winkler modulus parameter

To study the influence of the side-to-thickness ratio a/h and Winkler modulus k_w on the critical buckling temperature, Fig. 4 is presented. In this present computation, a constant value of the power law index, $k = 2$, is employed and the Pasternak shear modulus parameter is assumed as $k_g = 10$. From the figure it is observed that, regardless of the loading type, as the Winkler modulus parameter increases, the critical buckling temperature increases for all the different side-to-thickness ratio of FG square plate considered, especially for thicker plate. This implies that for embedded solar FG plate, there would be much shift of critical buckling temperature values from a soft elastic medium to a hard elastic medium. Moreover, it is observed that the change in critical

buckling temperature is more affected by the side-to-thickness ratios a/h. For a thin solar FG plate the effect of Winkler modulus on critical buckling temperature is less compared to thick solar FG plate.

3.2.3 Effect of Pasternak shear modulus parameter

Fig. 5 shows the effect of the side-to-thickness ratio a/h on the thermal buckling response of solar FG square plate with elastic medium modelled as Pasternak-type foundation. The Winkler

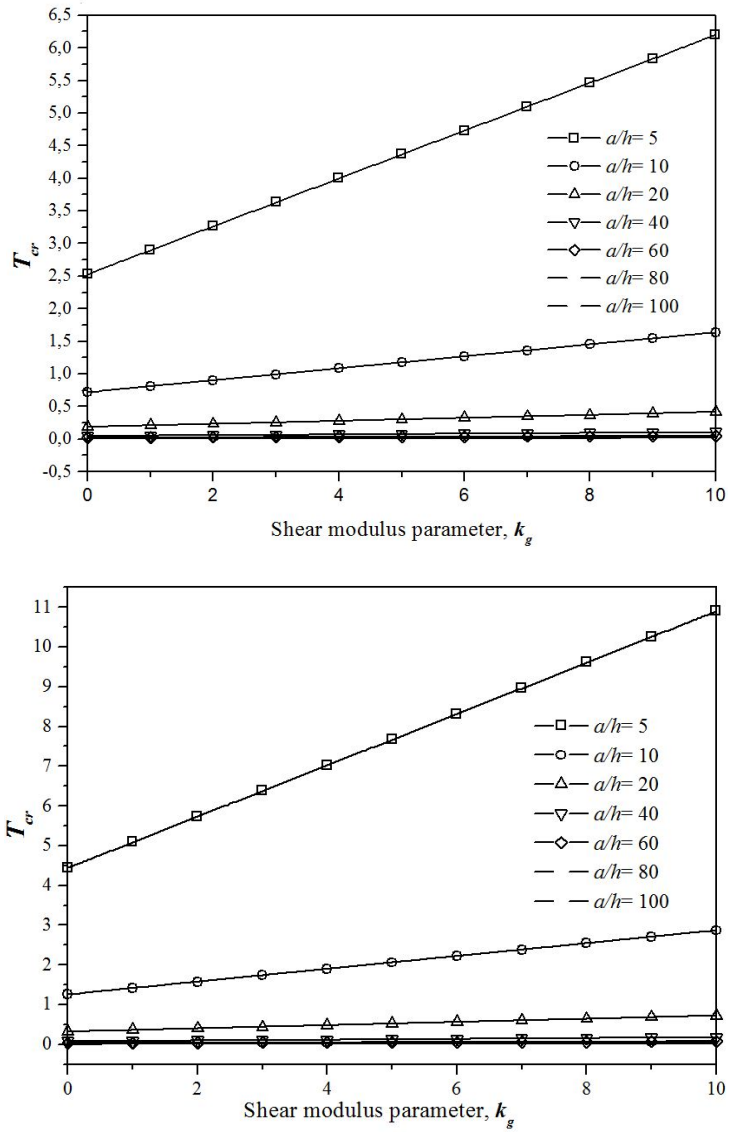

Fig. 5 Effect of Pasternak shear modulus parameter on the critical buckling temperature of square FG plate for various side-to-thickness ratios a/h with $k_g = 10$ and $k = 2$.
(a) Uniform temperature; (b) Linear temperature; (c) Non-linear temperature $\gamma = 3$

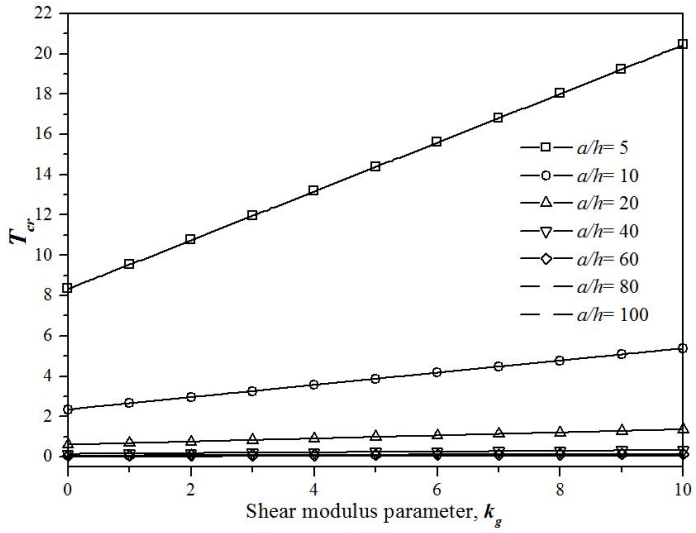

Fig. 5 Continued

modulus parameter is assumed as k_w = 10 and a constant value of the power law index k = 2, is employed. As the shear modulus parameter increases, the critical buckling temperature increases, especially for thicker plate and this regardless of the loading type. Like the variation of critical buckling temperature with stiffness parameter, considering Winkler-type foundation, the variation of critical buckling temperature considering Pasternak-type foundation is also linear in nature. In addition, it is observed, that change in critical buckling temperature is more affected by low side-to-thickness ratio values as seen in the Fig. 5.

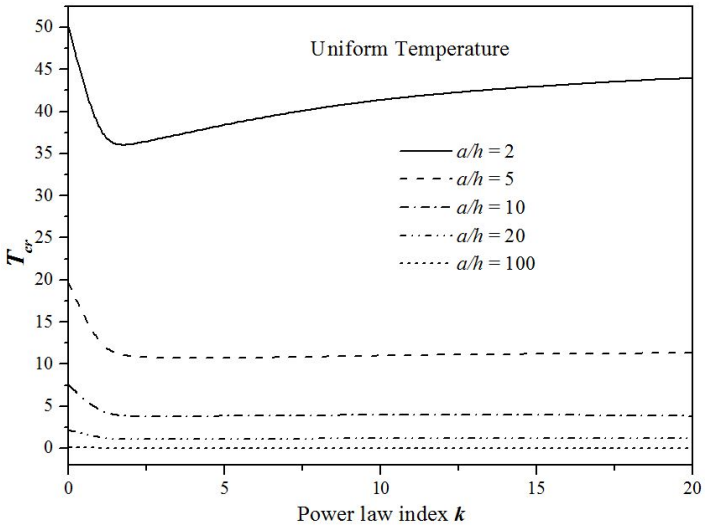

Fig. 6 Effect of power law index on the critical buckling temperature of square FG plate for various side-to-thickness ratios a/h with $k_w = k_g = 10$.
(a) Uniform temperature; (b) Linear temperature; (c) Non-linear temperature $\gamma = 3$

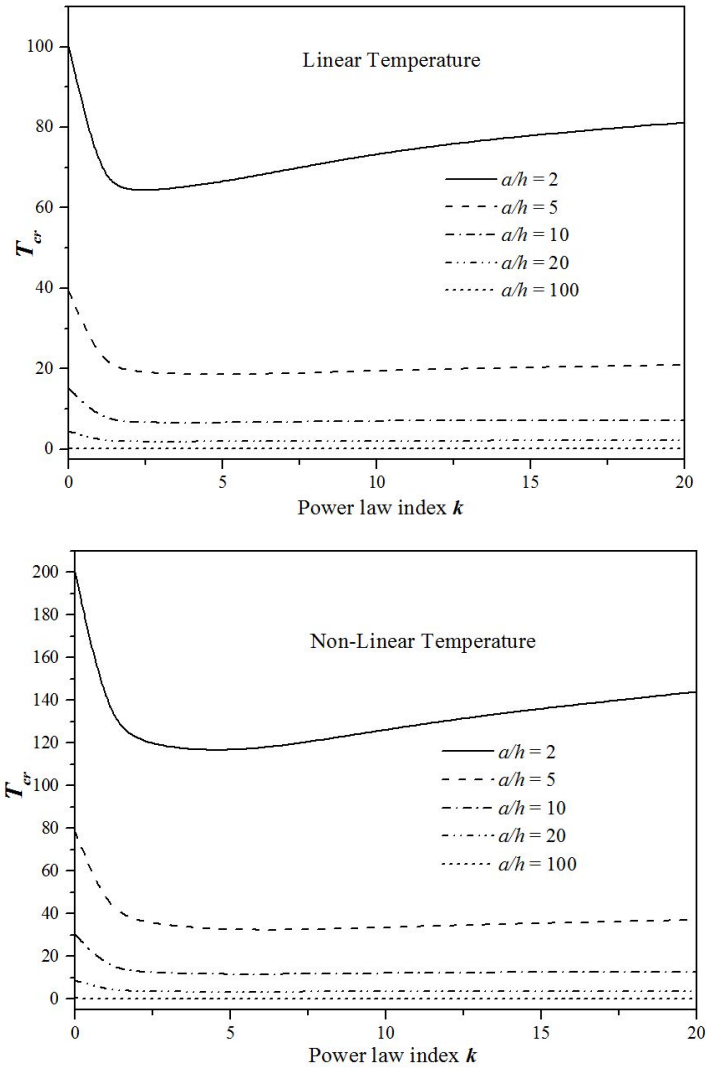

Fig. 6 Continued

3.2.4 Effect of the power law index on critical buckling temperature

To study the influence of the power law index k on the critical buckling temperature, Figs. 6 and 7 are presented for different side-to-thickness ratios a/h and aspect ratios a/b. It is assumed that the solar FG plate on elastic foundation with $k_w = k_g = 10$. It can be seen that in general the critical buckling temperature decreases as the power law index of solar FGM increases. This is due to the fact that increasing the power law index of solar FGM increases the volume fraction of metal. Furthermore, it can be found that the critical buckling temperature decreases with increasing the side-to-thickness ratios a/h. However, increasing the aspect ratio a/b, leads to an increase of the critical buckling temperature. It can be concluded that the performance of a solar FG plate in terms efficiency and service life depends on the material and operating conditions.

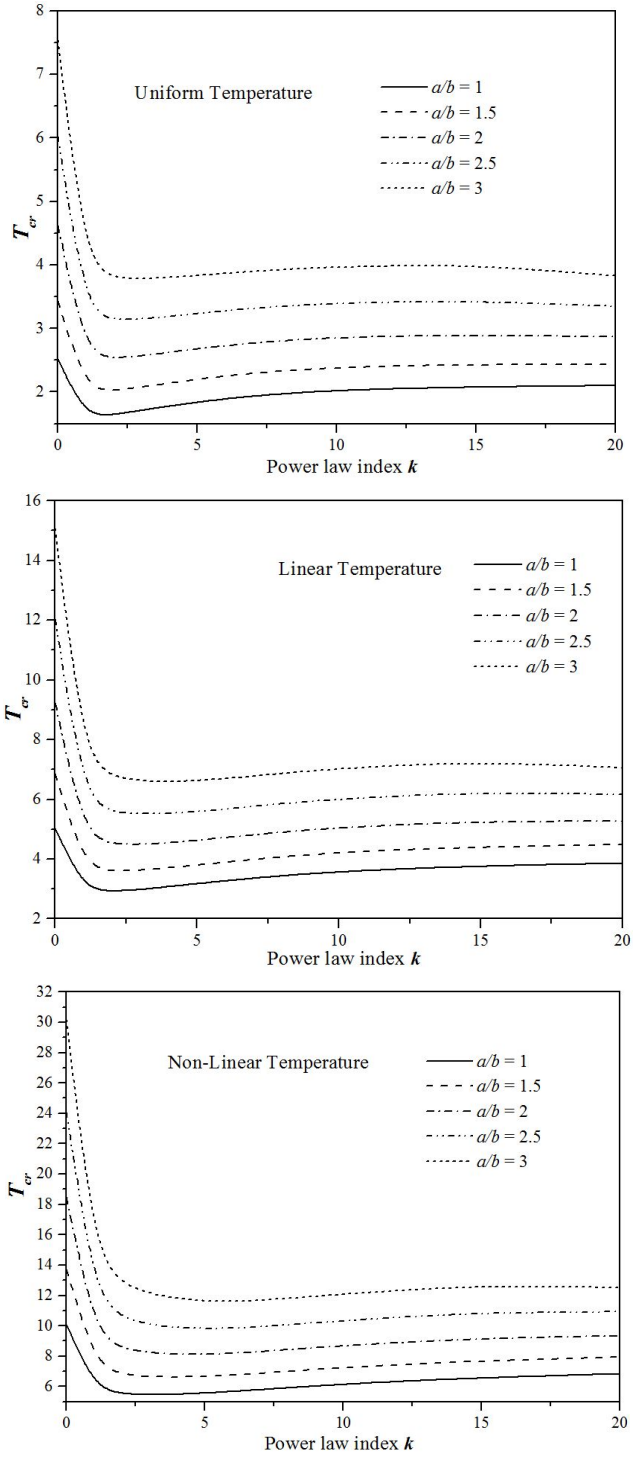

Fig. 7 Effect of power law index on the critical buckling temperature of FG plate (a/h = 10) for various aspect ratios a/h with $k_w = k_g = 10$.
(a) Uniform temperature; (b) Linear temperature; (c) Non-linear temperature $\gamma = 3$

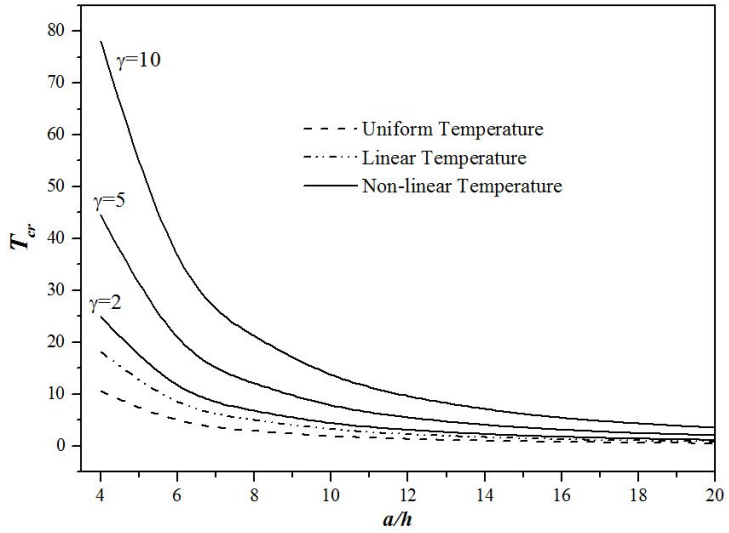

Fig. 8 Critical buckling temperature difference of FG square plate due to uniform, linear and non-linear temperature rise across the thickness versus the side-to-thickness ratio a/h with $k_w = k_g = 10$ and $k = 5$

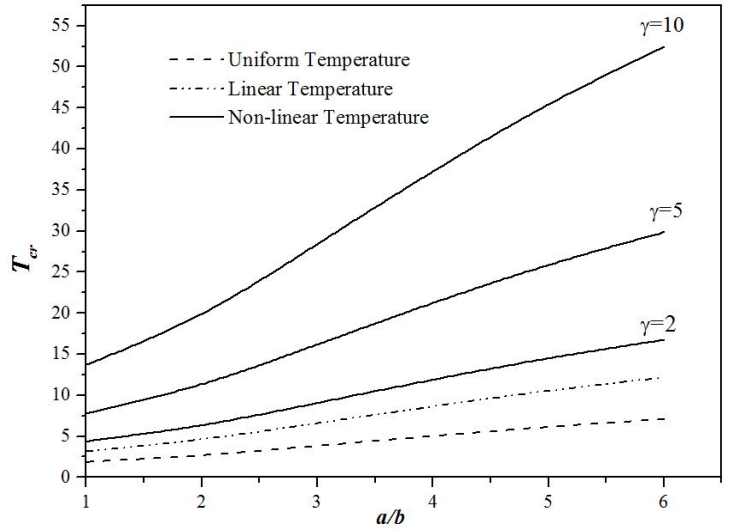

Fig. 9 Critical buckling temperature difference of FG plate (a/h = 10) due to uniform, linear and non-linear temperature rise across the thickness versus the aspect ratio a/b with $k_w = k_g = 10$ and $k = 5$

3.2.5 Effect of thermal loads types on critical buckling temperature

To examine the influence of thermal loads types on the critical buckling temperature, the variation of T_{cr} versus the side-to-thickness ratio a/h and aspect ratio a/b under various types of temperature loads is plotted in Figs. 8 and 9, respectively. It can be seen from Figs. 8 and 9 that T_{cr} of the solar plate under uniform temperature rise is smaller than that of the plate under linear temperature rise and the latter is smaller than that of the plate under non-linear temperature rise. In addition, it can be observed that T_{cr} is very sensitive to the variation of the temperature exponent γ.

4. Conclusions

In this research work, thermal buckling analysis of thick solar functionally graded rectangular plates resting on two-parameter foundation in thermal environment has been presented. The mechanical properties of the plate have been assumed to vary through the thickness of the plate as a power function. The neutral surface position for such plates has been determined. An efficient hyperbolic plate theory based on exact neutral surface position has been used to find the basic equations of solar FG plates on elastic foundation. The accuracy of the present theory is ascertained by comparing it with other higher-order shear deformation theories where an excellent agreement was observed in all cases. Furthermore, the influences of plate parameters such as power law index, aspect ratio, foundation stiffness coefficients and thermal loading types on the critical buckling temperature of solar FG rectangular plate have been comprehensively investigated. It can be concluded that the performance of a solar FG plate in terms efficiency and service life depends on the material and operating conditions.

Acknowledgments

This research was supported by the Algerian National Thematic Agency of Research in Science and Technology (ATRST) and university of Sidi Bel Abbes (UDL SBA) in Algeria.

References

Abdelhak, Z., Hadji, L., Daouadji, T.H. and Bedia, E.A. (2015), "Thermal buckling of functionally graded plates using a n-order four variable refined theory", *Adv. Mater. Res., Int. J.*, **4**(1), 31-44.

Abrate, S. (2008), "Functionally graded plates behave like homogeneous plates", *Compos. Part B*, **39**(1), 151-158.

Ait Amar Meziane, M., Abdelaziz, H.H. and Tounsi, A. (2014), "An efficient and simple refined theory for buckling and free vibration of exponentially graded sandwich plates under various boundary conditions", *J. Sandw. Struct. Mater.*, **16**(3), 293-318.

Ait Atmane, H., Tounsi, A. and Adda Bedia, E.A. (2010), "Free vibration analysis of functionally graded plates resting on Winkler–Pasternak elastic foundations using a new shear deformation theory", *Int. J. Mech. Mater. Des.*, **6**(2), 113-121.

Ait Atmane, H., Tounsi, A., Bernard, F. and Mahmoud, S.R. (2015), "A computational shear displacement model for vibrational analysis of functionally graded beams with porosities", *Steel Compos. Struct., Int. J.*, **19**(2), 369-384.

Ait Atmane, H., Tounsi, A. and Bernard, F. (2016), "Effect of thickness stretching and porosity on mechanical response of a functionally graded beams resting on elastic foundations", *Int. J. Mech. Mater. Des.*, 1-14.

Ait Yahia, S., Ait Atmane, H., Houari, M.S.A. and Tounsi, A. (2015), "Wave propagation in functionally graded plates with porosities using various higher-order shear deformation plate theories", *Struct. Eng. Mech., Int. J.*, **53**(6), 1143-1165.

Akbaş, Ş.D. (2015), "Wave propagation of a functionally graded beam in thermal environments", *Steel Compos. Struct., Int. J.*, **19**(6), 1421-1447.

Akil, A. (2014), "Post buckling analysis of sandwich beams with functionally graded faces using a consistent higher order theory", *Int. J. Civil Struct. Environ. Infrastr. Eng. Res. Develop.*, **4**(2), 59-64.

Al-Basyouni, K.S., Tounsi, A. and Mahmoud, S.R. (2015), "Size dependent bending and vibration analysis of functionally graded micro beams based on modified couple stress theory and neutral surface position", *Compos. Struct.*, **125**, 621-630.

Arefi, M. (2015), "Elastic solution of a curved beam made of functionally graded materials with different cross sections", *Steel Compos. Struct., Int. J.*, **18**(3), 569-672.

Attia, A., Tounsi, A., Adda Bedia, E.A. and Mahmoud, S.R. (2015), "Free vibration analysis of functionally graded plates with temperature-dependent properties using various four variable refined plate theories", *Steel Compos. Struct., Int. J.*, **18**(1), 187-212.

Bakora, A. and Tounsi, A. (2015), "Thermo-mechanical post-buckling behavior of thick functionally graded plates resting on elastic foundations", *Struct. Eng. Mech., Int. J.*, **56**(1), 85-106.

Belabed, Z., Houari, M.S.A., Tounsi, A., Mahmoud, S.R. and Anwar Bég, O. (2014), "An efficient and simple higher order shear and normal deformation theory for functionally graded material (FGM) plates", *Compos. Part B*, **60**, 274-283.

Belkorissat, I., Houari, M.S.A., Tounsi, A., Adda Bedia, E.A. and Mahmoud, S.R. (2015), "On vibration properties of functionally graded nano-plate using a new nonlocal refined four variable model", *Steel Compos. Struct., Int. J.*, **18**(4), 1063-1081.

Benachour, A., Daouadji, H.T., Ait Atmane, H., Tounsi, A. and Meftah, S.A. (2011), "A four variable refined plate theory for free vibrations of functionally graded plates with arbitrary gradient", *Compos. Part B*, **42**(6), 1386-1394.

Bennai, R., Ait Atmane, H. and Tounsi, A. (2015), "A new higher-order shear and normal deformation theory for functionally graded sandwich beams" *Steel Compos. Struct., Int. J.*, **19**(3), 521-546.

Bennoun, M., Houari, M.S.A. and Tounsi, A. (2016), "A novel five variable refined plate theory for vibration analysis of functionally graded sandwich plates", *Mech. Adv. Mater. Struct.*, **23**(4), 423-431.

Benyoucef, S., Tounsi, A., Fekrar, A., Ait Atmane, H. and Adda Bedia, E.A. (2010), "Bending of thick functionally graded plates resting on Winkler–Pasternak elastic foundations", *Mech. Compos. Mater.*, **46**(4), 425-434.

Besseghier, A., Heireche, H., Bousahla, A.A., Tounsi, A. and Benzair, A. (2015), "Nonlinear vibration properties of a zigzag single-walled carbon nanotube embedded in a polymer matrix", *Adv. Nano Res., Int. J.*, **3**(1), 29-37.

Bouazza, M., Tounsi, A., Adda-Bedia, E.A. and Megueni, A. (2010), "Thermoelastic stability analysis of functionally graded plates: An analytical approach", *Computat. Mater. Sci.*, **49**(4), 865-870.

Bouchafa, A., Bachir Bouiadjra, M., Houari, M.S.A. and Tounsi, A. (2015), "Thermal stresses and deflections of functionally graded sandwich plates using a new refined hyperbolic shear deformation theory", *Steel Compos. Struct., Int. J.*, **18**(6), 1493-1515.

Bouderba, B., Houari, M.S.A. and Tounsi, A. (2013), "Thermomechanical bending response of FGM thick plates resting on Winkler–Pasternak elastic foundations", *Steel Compos. Struct., Int. J.*, **14**(1), 85-104.

Bounouara, F., Benrahou, K.H., Belkorissat, I. and Tounsi, A. (2016), "A nonlocal zeroth-order shear deformation theory for free vibration of functionally graded nanoscale plates resting on elastic foundation", *Steel Compos. Struct., Int. J.*, **20**(2), 227-249.

Bourada, M., Tounsi, A., Houari, M.S.A. and Adda Bedia, E.A. (2012), "A new four-variable refined plate theory for thermal buckling analysis of functionally graded sandwich plates", *J. Sandw. Struct. Mater.*, **14**(1), 5-33.

Bourada, M., Kaci, A., Houari, M.S.A. and Tounsi, A. (2015), "A new simple shear and normal deformations theory for functionally graded beams", *Steel Compos. Struct., Int. J.*, **18**(2), 409-423.

Bousahla, A.A., Houari, M.S.A., Tounsi, A. and Adda Bedia, E.A. (2014), "A novel higher order shear and normal deformation theory based on neutral surface position for bending analysis of advanced composite plates", *Int. J. Computat. Method.*, **11**(6), 1350082.

Chattibi, F., Benrahou, K.H., Benachour, A., Nedri, K. and Tounsi, A. (2015), "Thermomechanical effects on the bending of antisymmetric cross-ply composite plates using a four variable sinusoidal theory", *Steel Compos. Struct., Int. J.*, **19**(1), 93-110.

Darılmaz, K. (2015), "Vibration analysis of functionally graded material (FGM) grid systems", *Steel Compos. Struct., Int. J.*, **18**(2), 395-408.

Draiche, K., Tounsi, A. and Khalfi, Y. (2014), "A trigonometric four variable plate theory for free vibration of rectangular composite plates with patch mass", *Steel Compos. Struct., Int. J.*, **17**(1), 69-81.

Ebrahimi, F. and Dashti, S. (2015)," Free vibration analysis of a rotating non-uniform functionally graded beam", *Steel Compos. Struct., Int. J.*, **19**(5), 1279-1298.

Fekrar, A., Houari, M.S.A., Tounsi, A. and Mahmoud, S.R. (2014), "A new five-unknown refined theory based on neutral surface position for bending analysis of exponential graded plates", *Meccanica*, **49**(4), 795-810.

Ganapathi, M. and Prakash, T. (2006), "Thermal buckling of simply supported functionally graded skew plates", *Compos. Struct.*, **74**(2), 247-250.

Hadji, L., Daouadji, T.H., Tounsi, A. and Bedia, E.A. (2014), "A higher order shear deformation theory for static and free vibration of FGM beam", *Steel Compos. Struct., Int. J.*, **16**(5), 507-519.

Hadji, L., Hassaine Daouadji, T., Tounsi, A. and Adda Bedia, A. (2015), "A n-order refined theory for bending and free vibration of functionally graded beams", *Struct. Eng. Mech., Int. J.*, **54**(5), 923-936.

Hamidi, A., Houari, M.S.A., Mahmoud, S.R. and Tounsi, A. (2015), "A sinusoidal plate theory with 5-unknowns and stretching effect for thermomechanical bending of functionally graded sandwich plates", *Steel Compos. Struct., Int. J.*, **18**(1), 235-253.

Hebali, H., Tounsi, A., Houari, M.S.A., Bessaim, A. and Adda Bedia, E.A. (2014), "A new quasi-3D hyperbolic shear deformation theory for the static and free vibration analysis of functionally graded plates", *ASCE J. Eng. Mech.*, **140**(2), 374-383.

Howell, A. and Bereny, J. (1979), *Engineer's Guide to Solar Energy*, Solar Energy Information Services, USA.

Kar, V.R. and Panda, S.K. (2015), "Nonlinear flexural vibration of shear deformable functionally graded spherical shell panel", *Steel Compos. Struct., Int. J.*, **18**(3), 693-709.

Khalfi, Y., Houari, M.S.A. and Tounsi, A. (2014), "A refined and simple shear deformation theory for thermal buckling of solar functionally graded plates on elastic foundation", *Int. J. Computat. Method.*, **11**(5), 135007.

Kiani, Y. and Eslami, M.R. (2012), "Thermal buckling and post-buckling response of imperfect temperature-dependent sandwich FGM plates resting on elastic foundation", *Arch. Appl. Mech.*, **82**(7), 891-905.

Koizumi, M. (1997), "FGM Activities in Japan", *Compos. Part B*, **28**(1-2), 1-4.

Larbi Chaht, F., Kaci, A., Houari, M.S.A., Tounsi, A., Anwar Bég, O. and Mahmoud, S.R. (2015), "Bending and buckling analyses of functionally graded material (FGM) size-dependent nanoscale beams including the thickness stretching effect", *Steel Compos. Struct., Int. J.*, **18**(2), 425-442.

Lanhe, W. (2004), "Thermal buckling of a simply supported moderately thick rectangular FGM plate," *Compos. Struct.*, **64**(2), 211-218.

Mahi, A., Adda Bedia, E.A. and Tounsi, A. (2015), "A new hyperbolic shear deformation theory for bending and free vibration analysis of isotropic, functionally graded, sandwich and laminated composite plates", *Appl. Math. Model.*, **39**(9), 2489-2508.

Matsunaga, H. (2009), "Thermal buckling of functionally graded plates according to a 2D higher-order deformation theory", *Compos. Struct.*, **90**(1), 76-86.

Meradjah, M., Kaci, A., Houari, M.S.A., Tounsi, A. and Mahmoud, S.R. (2015), "A new higher order shear and normal deformation theory for functionally graded beams", *Steel Compos. Struct., Int. J.*, **18**(3), 793-809.

Morimoto, T., Tanigawa, Y. and Kawamura, R. (2006), "Thermal buckling of functionally graded rectangular plates subjected to partial heating", *Int. J. Mech. Sci.*, **48**(9), 926-937.

Na, K.S. and Kim, J.H. (2006), "Thermal postbuckling investigations of functionally graded plates using 3-D finite element method", *Finite Elem. Anal. Des.*, **42**(8-9), 749-756.

Nguyen, K.T., Thai, T.H. and Vo, T.P. (2015), "A refined higher-order shear deformation theory for bending, vibration and buckling analysis of functionally graded sandwich plates", *Steel Compos. Struct., Int. J.*, **18**(1), 91-120.

Ould Larbi, L, Kaci, A., Houari, M.S.A. and Tounsi, A. (2013), "An efficient shear deformation beam theory based on neutral surface position for bending and free vibration of functionally graded beams", *Mech. Base. Des. Struct. Mach.*, **41**(4), 421-433.

Pasternak, P.L. (1954), "On a new method of analysis of an elastic foundation by means of two foundation constants", *Gosuedarstvennoe Izadatelstvo Literatim po Stroitelstvu i Arkhitekture*, **1**, 1-56.

Pradhan, K.K. and Chakraverty, S. (2015), "Free vibration of functionally graded thin elliptic plates with various edge supports", *Struct. Eng. Mech., Int. J.*, **53**(2), 337-354.

Reddy, J.N. (2000), "Analysis of functionally graded plates", *Int. J. Numer. Method. Eng.*, **47**(1-3), 663-684.

Saidi, A.R. and Jomehzadeh, E. (2009), "On analytical approach for the bending/stretching of linearly elastic functionally graded rectangular plates with two opposite edges simply supported", *Proc. IMechE, Part C: J. Mech. Eng. Sci.*, **223**(9), 2009-2016.

Salima, A., Fekrar, A., Heireche, H., Saidi, H., Tounsi, A. and Adda Bedia, E.A. (2016), "An efficient and simple shear deformation theory for free vibration of functionally graded rectangular plates on Winkler–Pasternak elastic foundations", *Wind Struct., Int. J.*, **17**(3), 329-348.

Sallai, B., Hadji, L., Hassaine Daouadji, T. and Adda Bedia, E.A. (2015), "Analytical solution for bending analysis of functionally graded beam", *Steel Compos. Struct., Int. J.*, **19**(4), 829-841.

Samsam Shariat, B.A. and Eslami, M.R. (2007), "Buckling of thick functionally graded plates under mechanical and thermal loads", *Compos. Struct.*, **78**(3), 433-439.

Shahrjerdi, A., Bayat, M., Mustapha, F., Sapuan, S.M. and Zahari, R. (2010), "Second order shear deformation theory to analyze stress distribution for solar functionally graded plates", *Mech. Des. Struct. Mach.*, **38**(3), 348-361.

Shahrjerdi, A., Mustapha, F., Bayat, M. and Majid, D.L.A. (2011a), "Free vibration analysis of solar functionally graded plates with temperature-dependent material properties using second order shear deformation theory", *J. Mech. Sci. Technol.*, **25**(9), 2195-2209.

Shahrjerdi, A., Mustapha, F., Sapuan, S.M., Bayat, M., Abdul Majid, D.L.A. and Zahari, R. (2011b), "Thermal free vibration analysis of temperature-dependent functionally graded plates using second order shear deformation", *Key Eng. Mater.*, **471-472**, 133-139.

Sobhy, M. (2013), "Buckling and free vibration of exponentially graded sandwich plates resting on elastic foundations under various boundary conditions", *Compos. Struct.*, **99**, 76-87.

Suresh, S. and Mortensen, A. (1998), *Fundamentals of Functionally Graded Materials*, IOM Communications Ltd., London, UK.

Tagrara, S.H., Benachour, A., Bachir Bouiadjra, M. and Tounsi, A. (2015), "On bending, buckling and vibration responses of functionally graded carbon nanotube-reinforced composite beams", *Steel Compos. Struct., Int. J.*, **19**(5), 1259-1277.

Talha, M. and Singh, B.N. (2010), "Static response and free vibration analysis of FGM plates using higher order shear deformation theory", *Appl. Math. Model*, **34**(12), 3991-4011.

Tebboune, W., Benrahou, K.H., Houari, M.S.A. and Tounsi, A. (2015), "Thermal buckling analysis of FG plates resting on elastic foundation based on an efficient and simple trigonometric shear deformation theory", *Steel Compos. Struct., Int. J.*, **18**(2), 443-465.

Tounsi, A., Houari, M.S.A., Benyoucef, S. and Adda Bedia, E.A. (2013), "A refined trigonometric shear deformation theory for thermoelastic bending of functionally graded sandwich plates", *Aerosp. Sci. Technol.*, **24**(1), 209-220.

Winkler, E. (1867), "Die lehre von der elasticitaet und festigkeit", Prag Dominicus.

Yaghoobi, H. and Torabi, M. (2013), "Exact solution for thermal buckling of functionally graded plates resting on elastic foundations with various boundary conditions", *J. Therm. Stress.*, **36**(9), 869-894.

Yaghoobi, H., Valipour, M.S., Fereidoon, A. and Khoshnevisrad, P. (2014), "Analytical study on post-buckling and nonlinear free vibration analysis of FG beams resting on nonlinear elastic foundation under thermo-mechanical loadings using VIM", *Steel Compos. Struct., Int. J.*, **17**(5), 753-776.

Zenkour, A.M. (2009), "The refined sinusoidal theory for FGM plates on elastic foundations", *Int. J. Mech. Sci.*, **51**(11-12), 869-880.

Zenkour, A.M. and Abouelregal, A.E. (2015), "Thermoelastic interaction in functionally graded nanobeams subjected to time-dependent heat flux", *Steel Compos. Struct., Int. J.*, **18**(4), 909-924.

Zenkour, A.M. and Sobhy, M. (2010), "Thermal buckling of various types of FGM sandwich plates", *Compos. Struct.*, **93**(1), 93-102.

Zenkour, A.M. and Sobhy, M. (2011), "Thermal buckling of functionally graded plates resting on elastic foundations using the trigonometric theory", *J. Therm. Stress.*, **34**(11), 1119-1138.
Zenkour, A.M., Allam, M.N.M. and Radwan, A.F. (2014), "Effects of transverse shear and normal strains on FG plates resting on elastic foundations under hygro-thermo-mechanical loading", *Int. J. Appl. Mech.*, **6**(5), 1450063.
Zhang, D.G. and Zhou, Y.H. (2008), "A theoretical analysis of FGM thin plates based on physical neutral surface", *Computat. Mater. Sci.*, **44**(2), 716-720.
Zhao, X. and Liew, K.M. (2009), "Geometrically nonlinear analysis of functionally graded plates using the element-free kp-Ritz method", *Comput. Meth. Appl. Mech. Eng.*, **198**(33-36), 2796-2811.
Zhao, X., Lee, Y.Y. and Liew, K.M. (2009), "Mechanical and thermal buckling analysis of functionally graded plates", *Compos. Struct.*, **90**(2), 161-171.
Zidi, M., Tounsi, A., Houari, M.S.A., Adda Bedia, E.A. and Anwar Bég, O. (2014), "Bending analysis of FGM plates under hygro-thermo-mechanical loading using a four variable refined plate theory", *Aerosp. Sci. Technol.*, **34**, 24-34.

CC